PEI@SiO$_2$: synthesis from diatomite and application for capturing phenolic compounds from aqueous solution†

Zheng-Yong Chen, Ya-Yuan He and Hong-Wen Gao*

A "dissolving and rebuilding" method was applied to prepare a diatomiteethyleneimine–polymer (PEI) hybrid composite, and its structure and topography were characterized by XRD, SEM, TEM, FTIR, DTG, elemental analysis and ζ-potential. The results indicated that the PEI was efficiently assembled into the SiO$_2$ framework formed from diatomite. Attempts were made to use the composite to remove phenolic pollutants, *e.g.* phenol, *o*-chlorophenol and bisphenol A (BPA), from aqueous solution. These adsorptions were to be in accordance with lipid–water-partition law, and their K_{aw} values were calculated to be 79.1 L kg^{-1} for phenol, 37.3 L kg^{-1} for *o*-chlorophenol and 24.2 L kg^{-1} for BPA.

1. Introduction

Phenolic compounds are almost ubiquitous contaminants because of their widespread appearance in wastewater from discharged oil refineries, the paint, drug and pesticide industries, as the intermediates of processes.[1] The potential toxicity of phenol derivatives has received increasing attention, and some have been proven to be toxic.[2–5] For example, bisphenol A (BPA) can cause damage to the reproductive system and can affect cellular development.[5–7] Chlorophenol may cause inflammation in the digestive system and increase blood pressure.[8] Because of their toxicity, phenolic compounds incorporate two classes of compounds widely prevalent and classified by the US Environmental Protection Agency as priority pollutants.[9] As per the recommendation of the World Health Organization, the threshold concentration of phenol in drinking water should fall below 1.0 μg L^{-1}.[10]

During recent decades, there has been significant interest in development of efficient techniques for removal of highly toxic organic compounds such as pesticides, fertilizers, hydrocarbons, phenols and plasticizers, from wastewater.[11–14] The adsorption technique was quite popular because of its simplicity, as well as the availability of a wide range of adsorbents.[15,16] For adsorption of phenolic compounds from aqueous solution, various adsorbents such as granular activated carbon and fibrous activated carbon,[17] mesoporous alumina-aluminum phosphates,[18] synthetic polymers[19] and ion exchange resins,[20] have been used. In recent years, a strategy to remove organic

pollutants using natural minerals was developed owing to their flexibility, general applicability and low cost.[21–23] However, low adsorption capacity and poor selectivity restrict application of original natural minerals.[24] Recently, further efforts in chemical modification of the pristine minerals have offered new possibilities for preparation of new materials with superior performances for a variety of applications. For instance, Bhardwaj *et al.* modified clinoptilolite and zeolite Y for adsorbing 2,4-dichlorophenoxyacetic acid,[25] and Xie *et al.* demonstrated a versatile chitosan modified zeolite for removal of different pollutants from water.[26] So far, impregnation, acid pickling, calcining and ionic exchange have been employed to modify natural pristine minerals. However, the conventional surface modification usually brings out some serious defects, for example unapparent improvement in adsorption capacity and easy separation of active group.[10,27,28]

PEI, which is composed of a large number of primary and secondary amine groups,[29] exhibits outstanding adsorption ability for various pollutants,[30,31] *e.g.* carbon dioxide,[32] heavy metals[29,33] and phenols.[34] Diatomite is known as an adsorbent for pollution control.[35–37] It can be dissolved easily to form abundant amorphous silica (SiO$_2$·nH$_2$O) under hydrothermal conditions. In previous papers, mesoporous materials, such as MCM-41,[38–41] mordenite[42] and ZSM-5 zeolites,[43,44] have been obtained from natural diatomite under hydrothermal conditions. Thus it is possible to turn diatomite and PEI into a multifunctional hybrid adsorbent for phenols using a "dissolving and rebuilding" method.

In the present work, an innovative approach, *i.e.* dissolving and rebuilding, was used to prepare a hybrid composite PEI@SiO$_2$ by dissolving PEI in the diatomite alkaline solution. As an excellent sorbent, it was used to adsorb phenolic compounds with a high adsorption capacity. The simple

State Key Laboratory of Pollution Control and Resource Reuse, College of Environmental Science and Engineering, Tongji University, Shanghai 200092, China. E-mail: hwgao@tongji.edu.cn; Fax: +86-21-65988598; Tel: +86-21-65988598

synthesis overcomes the disadvantages of traditional surface modification.

2. Experimental

2.1 Apparatus and materials

A photodiode array spectrometer (Model S4100, Scinco, Korea) was used to determine phenolic compounds in aqueous solutions. The concentrations of mixed phenolic compounds in the supernatants were measured by high-performance liquid chromatography (HPLC) with a DAD detector (Model LC 2000, Hitachi, Japan). The elemental analysis device (Model Vario EL III, Germany) was used to determine C, N and H contents of the hybrid composite. The microstructure and morphology of the material were measured by scanning electronic microscopy (SEM) (Model Quanta 200 FEG, FEI Co., USA) and transmission electron microscopy (TEM) with an energy dispersive X-ray detector (Model TECNAI G2 S-TWIN, FEI Co., USA). The FT-IR spectra of the hybrid composite were obtained, using an infrared spectrometer system (Model Equinoxss/hyperion 2000, BRUKER Co., Germany). The X-ray diffraction (XRD) (Model Bruker D8 Advance, Germany) was recorded using CuK radiation in the range of $\sim$10–90° 2θ at 40 kV and 40 mA. A thermal analysis system (Model Q600 SDT Simultaneous DSC/TGA, TA instruments, USA) was used for thermogravimetry analysis (TGA) of the materials. A ζ-potential instrument (Zetasizer Nano Z, Malvern, UK) was used to determine the surface potential of the PEI@SiO$_2$ composite. An inductively coupled plasma optical emission spectrometer (ICP-OES) (Model Optima 2100 DV, PerkinElmer, USA) was used to determine metal contents in materials.

Diatomite (Aladdin Agents, China), sodium hydroxide (Aladdin Agents, China), PEI (M.W. 600, Aladdin Agents, China), sodium chloride (Aladdin Agents, China) and hydrochloric acid (Sinopharm Chemical Reagent Co., Ltd, China) were used. Three phenolic compounds, i.e. phenol, o-chlorophenol and BPA (Aladdin Agents, China), adsorbing on the PEI@SiO$_2$ were investigated. As, Bi, Cd, Cu, Cr, Fe, Hg, Mn, Ni, Se, Pb, Zn multi-element mixed standard solutions (100 ppm, Aladdin Agents, China) were used.

2.2 Synthesis and characterization of the PEI@SiO$_2$

Diatomite (20 g) was added to 1000 mL of 2 mol L^{-1} sodium hydroxide, and stirred at 500 rpm for 24 h at 363 K. The mixture was centrifuged to remove insoluble residue into the supernatant containing 17.66 g L^{-1} diatomite, 0.21 M PEI was added and the solution was adjusted to pH 10 with 1 M HCl under stirring. After 24 h, the PEI@SiO$_2$ suspension was centrifuged and washed for several times with deionized water. The PEI@SiO$_2$ product was dried and ground into powder for characterization of the structure, composition and morphology. The PEI content was calculated by determining C content with an elemental analysis device. The PEI@SiO$_2$ powder was digested with 2.0 M sodium hydroxide and Al, Fe and Si contents in the supernatant were determined by ICP-OES. Using the same

method, SiO$_2$-only product formed from diatomite was prepared where PEI was not added.

2.3 Adsorption of phenolic compounds

The adsorption capacity of the PEI@SiO$_2$ composite to three phenolic compounds was determined. Phenol solutions from 6 to 500 mg L^{-1} were treated with 0.3% of the PEI@SiO$_2$ composite. All of the liquids were mixed for 30 min at 500 rpm by a magnetic stirrer and then centrifuged to separate adsorbent residue. The phenol concentrations remaining in the supernatants were determined by UV spectrophotometry. Using the same method, o-chlorophenol solutions from 6 to 650 mg L^{-1} and BPA solutions from 3 to 400 mg L^{-1} were treated.

The influences of pH from 3 to 11, ionic strength from 0 to 0.25 M, temperature from 298 to 328 K and the mixing time from 0 to 30 min were investigated for three phenolic compounds adsorbing to the PEI@SiO$_2$ composite.

2.4 Treatment of phenolic wastewater and disposal of the waste

Three phenolic wastewaters containing 20 mg L^{-1} phenol, 42 mg L^{-1} o-chlorophenol and 38 mg L^{-1} BPA, respectively, were treated with the PEI@SiO$_2$ from 0.1 to 1.8%. The phenolic compound remaining in each supernatant was determined by UV spectrophotometry. In addition, their mixed solution was treated with the PEI@SiO$_2$ from 0.1 to 1.8%. The phenolic compounds in the supernatants were determined by high-performance liquid chromatography (HPLC) with a DAD detector (Model LC 2000, Hitachi, Japan), where phenol was detected at 270 nm at 5.64 min, o-chlorophenol at 275 nm at 6.56 min and BPA at 286 nm at 8.36 min. The flow phase consisted of CH$_3$OH and H$_2$O according to 50 : 50 (V : V) at 0.5 mL min^{-1} of the flow speed through a chromatographic column (Model Allsphere ODS-25 μm, length 250 mm). The injection volume was 20 μL.

The phenol–PEI@SiO$_2$ waste (20 g) produced as above was calcined for 6 h at 550 °C with a Muffle furnace (Model SXL-1008, Shanghai Jinghong Lab Equipments Co., China). The residue was ground into powder approximately being 200 mesh. The phenol–PEI@SiO$_2$ waste calcined (0.5% (w/v)) was added to the As, Bi, Cd, Cu, Cr, Fe, Mn, Ni, Se, Pb multi-element mixed standard solution (1 mg L^{-1}) at pH 5 under stirring for 2 h. After the mixtures were centrifuged, the removal rates of pollutants in the supernatants were determined by ICP.

3. Results and discussion

3.1 Interaction of PEI with diatomite

When hybridizing PEI with diatomite to prepare the PEI@SiO$_2$ composite, the hybridization amount of PEI increases with increase of the PEI dosage and then approaches equilibrium (Fig. 1A). Hybridization of PEI obeys the Langmuir isotherm model (Fig. 1B), i.e. $c_e/q_e = 1/K_l q_\infty + c_e/q_\infty$,[45] where c_e is the equilibrium molarity of PEI in mol L^{-1}, q_e is the amount of PEI embedding in diatomite in mg g^{-1}, q_∞ is the saturation hybridization amount of PEI in mg g^{-1} and K_l is the binding
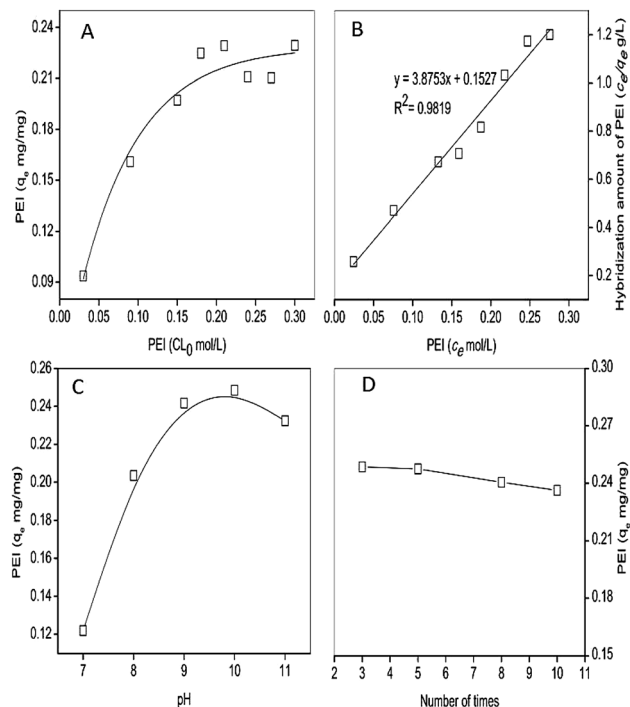
Fig. 1 Effect of PEI on hybridization. (A) Plots q_e vs. c_0, (B) plots c_e/q_e vs. c_e. (C) Effect of pH on hybridization of PEI. (D) Effect of water washing on the hybridization of PEI.

constant of PEI. The maximum PEI embedding in the PEI@SiO$_2$ composite approaches 258 mg g^{-1} and the K_1 is calculated to be 25.4 M^{-1}. A strong interaction, *i.e.* high affinity, occurs[34] between PEI and diatomite. The Gibbs free energy (ΔG) is less than zero, indicative of spontaneous interaction of the PEI@-SiO$_2$. The hybridization amount of PEI increases with increase of pH from 7 to 10 and then declines very slightly (Fig. 1C). Thus, preparation of the hybrid material is carried out at pH 10. Diatomite is hydrolyzed to form dissolved diatomite. Dissolved diatomite and PEI with initial weight ratio 1 : 7 are applied to prepare the PEI@SiO$_2$ at pH 10 (see the Experiment section).

The basic chain structure of PEI is the alkyl chain (–[CH$_2$–CH$_2$–NH]–$_n$), so there are a large number of nitrogen atoms of amino groups on the macromolecular chains of PEI. In aqueous solution, they may combine easily with H$^+$ to form –[CH$_2$–CH$_2$–NH$_2^+$]–$_n$,[11,46,47] which means that the majority of amino groups on PEI chains are protonated. The chain of PEI may be positively charged, *i.e.* forming cationic polyelectrolyte,[34] whereas diatomite particles are negatively charged, so both attract each other and PEI is adsorbed compactly to the surface of diatomite particles. The ζ-potential of diatomite-only is determined to be 34.0 mV in aqueous media, while that of the PEI@SiO$_2$ composite changes to +12.9 mV. After hybridizing, the electric property of the surface of diatomite changes substantially; it depends on the character of macromolecule PEI, so the surface of modified diatomite has a positive charge because of the strong acceptability of N atoms of PEI chains for protons. Thus, electrostatic interaction occurs between PEI$^+$ and diatomite.

It is well known that the main composition of diatomite is SiO$_2$ (88%), Al$_2$O$_3$ and Fe$_2$O$_3$.[48] The molar ratio of PEI to Si, Al and Fe is calculated as 1 : 248.5 : 61.8 : 2.6 in the PEI@SiO$_2$, which is determined by element analysis and ICP. This provides evidence for formation of the PEI@SiO$_2$ composite. Approximately 248.5 mg g^{-1} PEI is embedded in the composite, which is much more than reported elsewhere. In previous papers, Gao introduced an interesting study for modifying diatomite by PEI impregnation, and the maximum PEI embedding in the diatomite approached 128 mg g^{-1},[34] and Öztekin employed bentonite clay particles to adsorb PEI with the maximum of PEI embedding approaching 145 mg g^{-1}.[49] Thus the "dissolving and rebuilding" approach increases the hybridization capacity of PEI more than the conventional surface modification approach. In addition, easy migration of active groups and secondary pollution are some serious defects of conventional surface modification,[50,51] limiting its applications. PEI cannot be separated from the PEI@SiO$_2$ composite by washing with water (Fig. 1D), which shows that the "dissolving and rebuilding" approach exhibits better resistance to migration of active groups than does conventional surface modification. Therefore, the composite is suitable for treatment of wastewater.

3.2 Structure and morphology of the PEI@SiO$_2$

As shown in Fig. 2A, absorption peaks at 2935 (C–H stretching), 2819 (C–H stretching), 1756 (–NH$_2$ and –NH– deformation) and 1471 (–NH$_2$ and –NH– deformation) cm^{-1} indicate that PEI embedding in the PEI@SiO$_2$ composite is confirmed from its infrared spectra (IR). The Si–O absorption peak is at 1059 cm^{-1}. The XRD patterns for SiO$_2$-only and PEI@SiO$_2$ are shown in Fig. 2B. XRD patterns of SiO$_2$-only and PEI@SiO$_2$ all show a broad diffraction peak from $2\theta = 15$–$30°$, which indicates that SiO$_2$ holds mainly amorphous silica structure and there is no prominent difference caused by PEI in the PEI@SiO$_2$ composite,[52–54] that is the main structure of the hybrid composite remains unchanged. If there is a nanocrystalline silica material, corresponding peaks should be observed at a definite diffraction angle.[55] Similar work based on addition of ionic liquid coated sulfonic acid,[54] β-cyclodextrin[56] and nano-sized NiO particles[57] with functionalized amorphous silica composites has been reported with the prominent XRD peaks. As seen in the thermal gravimetric analysis (TGA) differential thermal gravity of PEI@SiO$_2$ (Fig. 2C), the first step in the range of 40–200 °C is attributed to removal of the physisorbed water and interlayer water.[58] Additional observed weight loss steps indicate the behavioral complexity of decomposition of the various covalently attached organic phases.[59] The second step in the range of 200–400 °C is caused by removal of the branched chain group of, and the third step in the range of 400–500 °C is caused by the removal of the straight chain of PEI. Similar TGA weight losses profiling also arose from previous reports.[59–61] The loss of weight between 200 °C and 500 °C indicates that approximately 25.3% PEI is embedded into the PEI@SiO$_2$ composite, which accords with the above reaction rate of PEI. From the differential thermogravimetry analysis (DTG) curves (Fig. 2C and S1, ESI†), a new peak appears at around 272 °C for
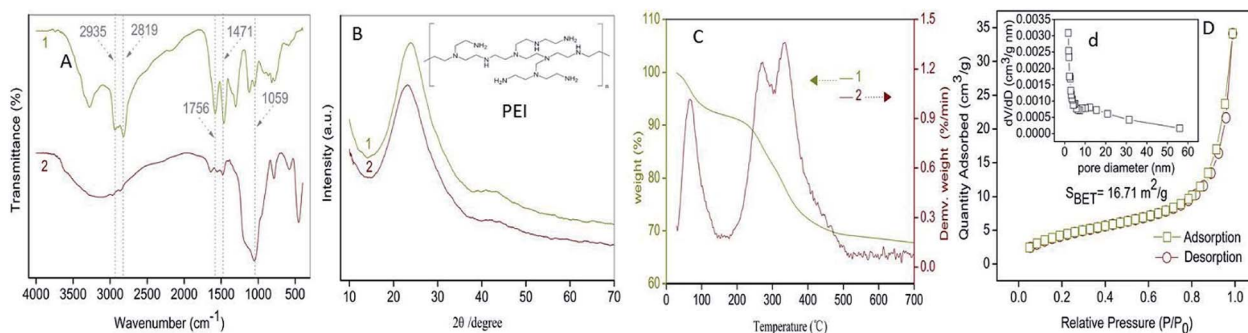
Fig. 2 IR spectra (A) of PEI (A1), the PEI@SiO$_2$ (A2) and XRD (B) of SiO$_2$-only (B1), the PEI@SiO$_2$ (B2), DTA of the PEI@SiO$_2$ (C1), TGA of the PEI@SiO$_2$ (C2) and N$_2$ absorption–desorption isotherm and pore-size distribution (inset) for PEI@SiO$_2$ (D, d).

the PEI@SiO$_2$ composite. This indicates the intermolecular interaction of PEI with SiO$_2$. Fig. 2D illustrates the N$_2$ sorption isotherm and the pore-size distribution with the Barrett–Joyner–Halenda method of PEI@SiO$_2$. The isotherm is classical type IV, which refers to the mesoporous materials. Furthermore, the isotherms have two hysteresis loops, indicating a bimodal pore size distribution in the mesoporous regions. At the high relative pressure between 0.8 and 0.9, the hysteresis loops are type H1, suggesting the presence of cylindrical mesopores.[62] The bimodal pore-size distribution is confirmed by the pore-size distribution in Fig. 4D. From the pore plots, no peak appeared in the pore, indicating the presence of irregular mesopores. The mesopores may be formed by the SiO$_2$. The BET analysis of the material indicates that the specific surface area of PEI@SiO$_2$ is determined to be 16.71 m^2 g^{-1}.

From the SEM images, diatomite consisting of the tiny aquatic organism remains fossilized (Fig. 3C). The PEI@SiO$_2$ particles are irregular in the size of 100–500 nm and stack-up of the reticular structure (Fig. 3A and B), where all the macropores (>50 nm) disappear (Fig. 3B). The pore size distribution (see Fig. S2, ESI†) is also similar for many amorphous silica studied.[63] The C, N, O, Al and Si are observed in the interior of the PEI@SiO$_2$ composite from the EDX (Fig. 3Aa). Just as one kind of adhesive, PEI is bridging among SiO$_2$ particles to change

the morphology of the PEI@SiO$_2$ composite (Fig. 3D). The stripes (red) of the SiO$_2$ particles and the irregular block (blue) of PEI are found (Fig. 3E). The lattice spacing of the crystal grain is 0.20 nm (Fig. 3F). This indicates the Al$_2$O$_3$ crystal grains (yellow) formed (Fig. 3E).

3.3 Adsorption of solo phenolic compounds on PEI@SiO$_2$

PEI contains lots of long hydrophobic chains so the PEI@SiO$_2$ composite carries a large amount of hydrophobicity. lg K_{ow} is the logarithm of the n-octanol–water partition coefficient, which underestimates the partition of organic compounds between n-octanol and water phases. It is well known that o-chlorophenol (lg K_{ow} = 3.06) and BPA (lg K_{ow} = 3.32) are
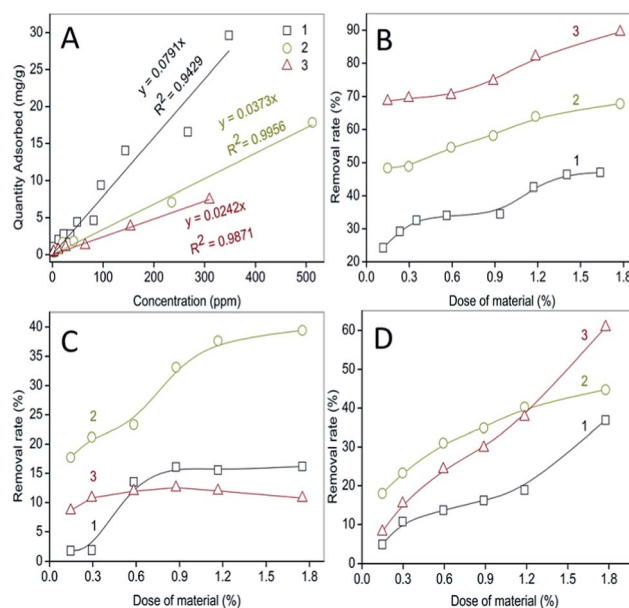

Fig. 4 (A) Adsorption of phenol (1), o-chlorophenol (2) and BPA (3) with PEI@SiO$_2$. (B) The removal rate of phenol (1), o-chlorophenol (2) and BPA (3) with PEI@SiO$_2$. Conditions-material dosage, 1.7–18 mg mL^{-1}. (C) The removal rate of phenol (1), o-chlorophenol (2) and BPA (3) with the diatomite. Conditions-material dosage, 1.7–18 mg mL^{-1}. (D) The removal rate of phenol (1), o-chlorophenol (2) and BPA (3) from their mixed solution with PEI@SiO$_2$. Conditions-material dosage, 1.5–18 mg mL^{-1}.
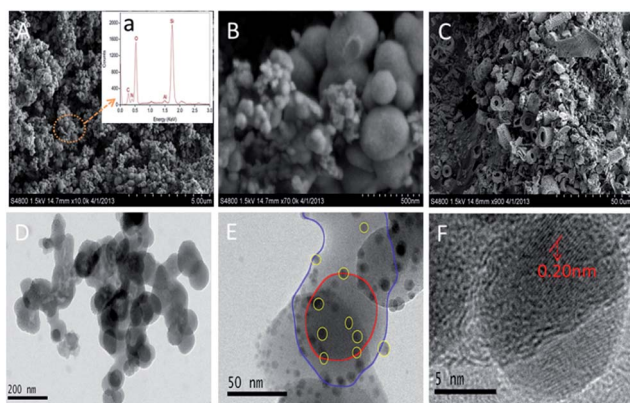

Fig. 3 SEM images of PEI@SiO$_2$ (A and B), diatomite (C), EDX of PEI@SiO$_2$ (Aa) and TEM of PEI@SiO$_2$ (D–F).

difficult to remove from water-drinking bodies by conventional methods, *e.g.* flocculation and disinfection.[64] A few studies have suggested that phenolic compounds can be adsorbed by sorbent through intermolecular acting force (mainly hydrophobic interaction).[34] Adsorption of phenol, *o*-chlorophenol and BPA in the PEI@SiO$_2$ composite is to accord with the lipid–water-partition law (Fig. 4A). The partition coefficient (K_{aw}) of phenol is calculated to be 79.1 L kg^{-1}, *i.e.* lg K_{aw} = 3.90, which is more than lg K_{ow}. In addition, lg K_{aw} = 1.38 for *o*-chlorophenol and 1.35 for BPA. The adsorption constant of phenol is $10^{-9.98}$. The benzene ring of the phenolic compounds may interact with the hydrophobic vinyl of PEI *via* a hydrophobic interaction. In addition, hydrogen bonds may form between PEI of the PEI@SiO$_2$ composite and phenol.

The adsorption equilibrium is completed in 10 min (Fig. S3A, ESI†), which is much faster than that of activated carbon and the other polymer sorbents.[65–68] It is considered that a hydrophobic interaction between adsorbent and organic compounds might be attributed to the rapid adsorption rate.[69] The rapid adsorption of phenolic compounds on PEI@SiO$_2$ ensures that sufficient time is available for adsorption equilibration to get at the usual operator condition of the adsorption. The pH of solution has not seriously affected the adsorption of those phenolic compounds (Fig. S3B, ESI†). However, in a previous paper, the adsorption capacities of diatomite with the conventional surface modification were very different under different conditions of pH values.[34] The sorption of phenolic compounds on diatomite modified by the conventional surface is the mode of monomolecular layer adsorption,[49,70,71] while the adsorption of phenolic compounds in PEI@SiO$_2$ composite is to accord with the lipid–water-partition law. Diatomite modified by the conventional surface interacts with phenolic compounds *via* hydrogen bond interaction, and the hydrogen bond interactions between PEI on diatomite surface and phenolic compounds are affected by the change of pH values.[34] However, PEI@SiO$_2$ interacts with phenolic compounds *via* the hydrophobic interaction and the hydrophobic interaction stays steady at different pH values. With ionic strength increasing from 0.05 to 0.2 mol L^{-1}, q_e of phenol, *o*-chlorophenol and BPA increase by 31.5%, 15.1% and 6.4%, respectively (Fig. S3C, ESI†). It is considered that the hydrogen bonding between phenolic compounds and H$_2$O becomes weak at higher ionic strength, which makes phenolic compound molecules freely available.[72–74] Hence, it is attributed that ionic strength can strengthen the hydrophobic interaction between phenolic compounds and PEI@SiO$_2$. Temperature is an important parameter for any separation process.[75] With the temperature increasing from 297 to 315 K, q_e of phenol decreases by 17.8%, while that of *o*-chlorophenol and BPA remains almost constant (Fig. S3D, ESI†). It is obvious the equilibrium adsorption capacity increases with increment of the equilibrium concentration but decreases with increasing temperature, suggesting that adsorption is favorable while an exothermic process.[76] A change in adsorption capacity with temperature is possibly because the adsorbate has a tendency to escape from the solid phase to the solution when the interaction is exothermic.[72]

3.4 Effect of adsorbent dosage

Effects of the PEI@SiO$_2$ composite's dosage were determined on adsorption of a mixture of three phenolic compounds (20 mg L^{-1} phenol, 42 mg L^{-1} *o*-chlorophenol and 38 mg L^{-1} BPA) and the results are shown in Fig. 4B and C. The removal rates of the three phenolic compounds increase with increasing dosage. The PEI@SiO$_2$ composite removed 47% phenol, 68% *o*-chlorophenol and 89% BPA; however, diatomite removed only 16% phenol, 39% *o*-chlorophenol and 11% BPA (Fig. 4B). Also, being different from the PEI@SiO$_2$ composite, diatomite adsorbing phenolic compounds obey the Freundlich model (Fig. 4C).[36,45] Therefore, diatomite interacting with phenolic compounds is different from the PEI@SiO$_2$ composite. The most possible reason is that the active group –O of diatomite interacted with phenolic compounds *via* hydrogen bonds. The PEI chain embedding into the PEI@SiO$_2$ composite bound to phenolic compounds *via* hydrophobic interaction.

The mixture solution of 20 mg L^{-1} phenol, 42 mg L^{-1} *o*-chlorophenol and 38 mg L^{-1} BPA is treated with the PEI@SiO$_2$ composite. From the results shown in Fig. 4D, 0.18% of the PEI@SiO$_2$ composite removed 37% phenol, 45% *o*-chlorophenol and 60% BPA. Compared with Fig. 4B, the adsorption of phenol, *o*-chlorophenol and BPA decreased by 21%, 34% and 33%, respectively. When three solutes compete for sorption in the trisolute system, the sorption amount of each solute is less than that in a single-solute system. It indicated that competitive adsorption occurred among the three phenolic compounds. As a result of limited active sites of the PEI@SiO$_2$, competitive hydrophobic interactions of the three phenolic compounds are expected to be the mechanism for inhibited desorption.[17,77]

3.5 Treatment of heavy metals with the phenol–PEI@SiO$_2$ waste calcined

To avoid secondary pollution and increase the comprehensive use of resource, recycling of spent materials is often necessary.[78] After the PEI@SiO$_2$ sludge with phenol is calcined at 550 °C, all organic compounds (phenol and PEI) are decomposed. The material calcined consists of SiO$_2$ and Al$_2$O$_3$, which is capable of
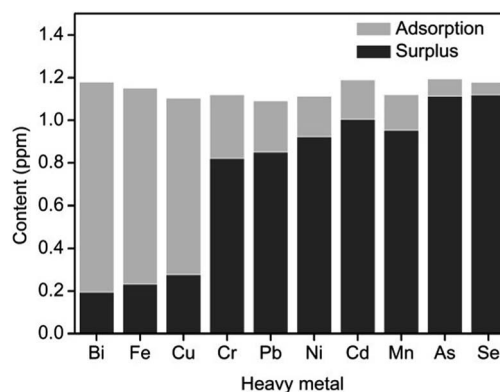

Fig. 5 The adsorption of multi-metals mixed with the phenol–PEI@SiO$_2$ waste calcined.

adsorbing metals.[79] The removal rates of Bi^{3+}, Fe^{3+} and Cu^{2+} are more than 75% (Fig. 5).

4. Conclusions

We have demonstrated an innovative method (dissolving and rebuilding) for producing hybrid adsorbent using natural mineral and organic polymer. Such a material has more hybrid amount of PEI, compared with reported materials.[34] More than 22.9% PEI is embedded so that the sorbent contains a large number of active sites, which results in exceptional adsorption capacity towards phenolic compounds. It conforms to the lipid–water-partition law and the K_{aw} of phenol, o-chlorophenol and BPA are 79.1 L kg^{-1}, 37.3 L kg^{-1} and 24.2 L kg^{-1}. After calcinations of the used PEI@SiO$_2$, the phenol–PEI@SiO$_2$ waste calcined exhibits a good sorption capacity to heavy metals and also can be used to eliminate heavy metal pollutant. This work has provided a novel approach for preparation of environmentally friendly inorganic–organic hybrids.

Notes and references

1 D. M. Nevskaia, E. Castillejos-Lopez, V. Munoz and A. Guerrero-Ruiz, *Environ. Sci. Technol.*, 2004, **38**, 5786–5796.

2 R. S. Juang, F. C. Wu and R. L. Tseng, *J. Chem. Eng. Data*, 1996, **41**, 487–492.

3 B. N. Estevinho, I. Martins, N. Ratola, A. Alves and L. Santos, *J. Hazard. Mater.*, 2007, **143**, 535–540.

4 M. O. Maebana, S. B. Mishra, B. B. Mamba and A. K. Mishra, *J. Appl. Polym. Sci.*, 2013, **128**, 2073–2080.

5 J. Y. Hu, T. Aizawa and Y. Magara, *Water Res.*, 1999, **33**, 417–425.

6 L. A. Jones and R. A. Hajek, *Environ. Health Perspect.*, 1995, **103**, 63–67.

7 A. Kortenkamp and R. Altenburger, *Sci. Total Environ.*, 1999, **233**, 131–140.

8 S. H. Song and M. Kang, *J. Ind. Eng. Chem.*, 2008, **14**, 785–791.

9 M. Sarkar and P. K. Acharya, *Waste Manage.*, 2006, **26**, 559–570.

10 M. Aivalioti, P. Papoulias, A. Kousaiti and E. Gidarakos, *J. Hazard. Mater.*, 2012, **207**, 117–127.

11 M. Amara and H. Kerdjoudj, *Desalination*, 2003, **155**, 79–87.

12 V. Kavitha and K. Palanivelu, *J. Photochem. Photobiol., A*, 2005, **170**, 83–95.

13 Y. X. Zhang, Z. L. Liu, B. Sun, W. H. Xu and J. H. Liu, *RSC Adv.*, 2013, **3**, 23197–23206.

14 Y. X. Zhang, X. Y. Yu, Z. Jin, Y. Jia, W. H. Xu, T. Luo, B. J. Zhu, J. H. Liu and X. J. Huang, *J. Mater. Chem.*, 2011, **21**, 16550–16557.

15 Y. Fukazawa, W. Pluemsab, N. Sakairi and T. Furuike, *Chem. Lett.*, 2005, **34**, 1652–1653.

16 H. El-Hamshary, S. El-Sigeny, M. F. Abou Taleb and N. A. El-Kelesh, *Sep. Purif. Technol.*, 2007, **57**, 329–337.

17 S. Kumar, M. Zafar, J. K. Prajapati, S. Kumar and S. Kannepalli, *J. Hazard. Mater.*, 2011, **185**, 287–294.

18 T. G. Danis, T. A. Albanis, D. E. Petrakis and P. J. Pomonis, *Water Res.*, 1998, **32**, 295–302.

19 D. Drechny and A. W. Trochimczuk, *React. Funct. Polym.*, 2006, **66**, 323–333.

20 S. Dutta, J. K. Basu and R. N. Ghar, *Sep. Purif. Technol.*, 2001, **21**, 227–235.

21 C. Volzone, *Appl. Clay Sci.*, 2007, **36**, 191–196.

22 V. K. Gupta, B. Gupta, A. Rastogi, S. Agarwal and A. Nayak, *Water Res.*, 2011, **45**, 4047–4055.

23 K. F. Lam, K. L. Yeung and G. McKay, *Environ. Sci. Technol.*, 2007, **41**, 3329–3334.

24 M. Rafatullah, O. Sulaiman, R. Hashim and A. Ahmad, *J. Hazard. Mater.*, 2010, **177**, 70–80.

25 D. Bhardwaj, P. Sharma, M. Sharma and R. Tomar, *RSC Adv.*, 2014, **4**, 4504–4514.

26 J. Xie, C. J. Li, L. A. Chi and D. Y. Wu, *Fuel*, 2013, **103**, 480–485.

27 A. F. D. de Namor, A. El Gamouz, S. Frangie, V. Martinez, L. Valiente and O. A. Webb, *J. Hazard. Mater.*, 2012, **241**, 14–31.

28 K. G. Bhattacharyya and S. Sen Gupta, *Adv. Colloid Interface Sci.*, 2008, **140**, 114–131.

29 Y. L. Chen, B. C. Pan, H. Y. Li, W. M. Zhang, L. Lv and J. Wu, *Environ. Sci. Technol.*, 2010, **44**, 3508–3513.

30 M. Ghoul, M. Bacquet and M. Morcellet, *Water Res.*, 2003, **37**, 729–734.

31 Y. Kuwahara, D.-Y. Kang, J. R. Copeland, N. A. Brunelli, S. A. Didas, P. Bollini, C. Sievers, T. Kamegawa, H. Yamashita and C. W. Jones, *J. Am. Chem. Soc.*, 2012, **134**, 10757–10760.

32 R. Sanz, G. Calleja, A. Arencibia and E. S. Sanz-Pérez, *J. Mater. Chem. A*, 2013, **1**, 1956–1962.

33 P. E. Duru, S. Bektas, O. Genc, S. Patir and A. Denizli, *J. Appl. Polym. Sci.*, 2001, **81**, 197–205.

34 B. J. Gao, P. F. Jiang, F. Q. An, S. Y. Zhao and Z. Ge, *Appl. Surf. Sci.*, 2005, **250**, 273–279.

35 M. Jang, S. H. Min, J. K. Park and E. J. Tlachac, *Environ. Sci. Technol.*, 2007, **41**, 3322–3328.

36 G. D. Sheng, S. T. Yang, J. Sheng, J. Hu, X. L. Tan and X. K. Wang, *Environ. Sci. Technol.*, 2011, **45**, 7718–7726.

37 M. A. M. Khraisheh, M. A. Al-Ghouti, S. J. Allen and M. N. Ahmad, *Water Res.*, 2005, **39**, 922–932.

38 Y. A. Cao, Q. H. Yuan, X. J. Mu, Y. Q. Xu and B. L. Liu, *Chin. J. Inorg. Chem.*, 2010, **26**, 2243–2250.

39 P. Yuan, D. Yang, Z. Y. Lin, H. P. He, X. Y. Wen, L. J. Wang and F. Deng, *J. Non-Cryst. Solids*, 2006, **352**, 3762–3771.

40 D. D. Li, H. Y. Min, X. Jiang, X. Q. Ran, L. Y. Zou and J. W. Fan, *J. Colloid Interface Sci.*, 2013, **404**, 42–48.

41 J. G. Shao, W. J. Deng, Y. X. Yang, X. N. Liu and Y. R. Chen, *Adsorpt. Sci. Technol.*, 2009, **27**, 147–165.

42 V. Sanhueza, U. Kelm and R. Cid, *J. Chem. Technol. Biotechnol.*, 2003, **78**, 485–488.

43 V. Sanhueza, L. Lopez-Escobar, U. Kelm and R. Cid, *J. Chem. Technol. Biotechnol.*, 2006, **81**, 614–617.

44 V. Sanhueza, U. Kelm, R. Cid and L. Lopez-Escobar, *J. Chem. Technol. Biotechnol.*, 2004, **79**, 686–690.

45 S. K. Parida, S. Dash, S. Patel and B. K. Mishra, *Adv. Colloid Interface Sci.*, 2006, **121**, 77–110.

46 M. Amara and H. Kerdjoudj, *Talanta*, 2003, **60**, 991–1001.

47 M. A. Andersson and R. Hatti-Kaul, *J. Biotechnol.*, 1999, **72**, 21–31.

48 S. Y. Shan, Q. M. Jia, L. H. Jiang, Q. C. Li, Y. M. Wang and J. H. Peng, *Ceram. Int.*, 2013, **39**, 5437–5441.

49 N. Öztekin, A. E. Alemdar, N. Gungor and F. B. Erim, *Mater. Lett.*, 2002, **55**, 73–76.

50 W. X. Zhao, Q. Ma, L. S. Li, X. R. Li and Z. L. Wang, *J. Adhes. Sci. Technol.*, 2014, **28**, 499–511.

51 J. Abenojar, R. Torregrosa-Coque, M. A. Martinez and J. M. Martin-Martinez, *Surf. Coat. Technol.*, 2009, **203**, 2173–2180.

52 N. Ghaemi, S. S. Madaeni, A. Alizadeh, H. Rajabi and P. Daraei, *J. Membr. Sci.*, 2011, **382**, 135–147.

53 J. Kim, S. J. Park and S. Kim, *J. Nanosci. Nanotechnol.*, 2012, **12**, 685–689.

54 P. Gupta, M. Kour, S. Paul and J. H. Clark, *RSC Adv.*, 2014, **4**, 7461.

55 H. Basri, A. F. Ismail and M. Aziz, *Desalination*, 2012, **287**, 71–77.

56 R. Nielsen, P. Kingshott, T. Uyar, J. Hacaloglu and K. L. Larsen, *Surf. Interface Anal.*, 2011, **43**, 884–892.

57 S. A. El-Safty, Y. Kiyozumi, T. Hanaoka and F. Mizukami, *Appl. Catal., A*, 2008, **337**, 121–129.

58 L. T. Zhuravlev, *Colloids Surf., A*, 2000, **173**, 1–38.

59 Y. K. Buchman, E. Lellouche, S. Zigdon, M. Bechor, S. Michaeli and J.-P. Lellouche, *Bioconjugate Chem.*, 2013, **24**, 2076–2087.

60 Y. Le, D. Guo, B. Cheng and J. Yu, *J. Colloid Interface Sci.*, 2013, **408**, 173–180.

61 S. Hammache, J. S. Hoffman, M. L. Gray, D. J. Fauth, B. H. Howard and H. W. Pennline, *Energy Fuels*, 2013, **27**, 6899–6905.

62 N. P. Wickramaratne and M. Jaroniec, *J. Mater. Chem. A*, 2013, **1**, 112.

63 G. Quercia, A. Lazaro, J. W. Geus and H. J. H. Brouwers, *Cem. Concr. Compos.*, 2013, **44**, 77–92.

64 Y. P. Wei and H. W. Gao, *J. Mater. Chem.*, 2012, **22**, 5715–5722.

65 L. Sun, C. G. Tian, L. Wang, J. L. Zou, G. Mu and H. G. Fu, *J. Mater. Chem.*, 2011, **21**, 7232–7239.

66 I. Y. Ipek, N. Kabay, M. Yuksel, D. Yapici and U. Yuksel, *Desalination*, 2012, **306**, 24–28.

67 C. Pacurariu, G. Mihoc, A. Popa, S. G. Muntean and R. Ianos, *Chem. Eng. J.*, 2013, **222**, 218–227.

68 G. Xu and H. Gao, *Acta Chim. Sin.*, 2012, **70**, 2496–2500.

69 M. Khalid, G. Joly, A. Renaud and P. Magnoux, *Ind. Eng. Chem. Res.*, 2004, **43**, 5275–5280.

70 M. Aivalioti, I. Vamvasakis and E. Gidarakos, *J. Hazard. Mater.*, 2010, **178**, 136–143.

71 P. Huttenloch, K. E. Roehl and K. Czurda, *Environ. Sci. Technol.*, 2001, **35**, 4260–4264.

72 D. M. Zhang, Z. L. Chen, J. M. Shen and L. Yang, *Water Sci. Technol.: Water Supply*, 2012, **12**, 259–269.

73 W. Wei, R. Sun, Z. Jin, J. Cui and Z. G. Wei, *Appl. Surf. Sci.*, 2014, **292**, 1020–1029.

74 L. Zhang, P. Fang, L. J. Yang, J. Zhang and X. Wang, *Langmuir*, 2013, **29**, 3968–3975.

75 M. N. Amin, A. I. Mustafa, M. I. Khalil, M. Rahman and I. Nahid, *Clean Technol. Environ.*, 2012, **14**, 837–844.

76 C. Y. Li, M. W. Xu, X. C. Sun, S. Han, X. F. Wu, Y. N. Liu, J. H. Huang and S. G. Deng, *Chem. Eng. J.*, 2013, **229**, 20–26.

77 E. Bayram, N. Hoda and E. Ayranci, *J. Hazard. Mater.*, 2009, **168**, 1459–1466.

78 P. Wang, Q. H. Shi, Y. F. Shi, K. K. Clark, G. D. Stucky and A. A. Keller, *J. Am. Chem. Soc.*, 2009, **131**, 182–188.

79 L. Charerntanyarak, *Water Sci. Technol.*, 1999, **39**, 135–138.